

Diurnal and day-to-day characteristics of ambient particle mass size distributions from HR-ToF-AMS measurements at an urban site and a suburban site in Hong Kong

Berto P. Lee¹, Hao Wang², and Chak K. Chan^{1,2*}

¹School of Energy and Environment, City University of Hong Kong, Hong Kong, China

²Division of Environment, Hong Kong University of Science and Technology, Hong Kong, China

Correspondence to: Chak K. Chan (chak.k.chan@cityu.edu.hk)

Abstract. Mass concentration based particle size distributions measured by a high-resolution aerosol mass spectrometer were systematically analyzed to assess long and short-term temporal characteristics of ambient particle size distributions sampled at a typical urban environment close to emission sources and a suburban coastal site representing a regional and local pollution receptor location in Hong Kong. Measured distributions were bimodal and deconvoluted into submodes which were analyzed for day-to-day variations and diurnal variations.

Traffic and cooking emissions at the urban site contributed substantially to particle mass in both modes, while notable decreases in mass median diameters were limited to the morning rush hour. Inorganic particle components displayed varying diurnal behavior, including nocturnal nitrate formation and daytime photochemical formation evident in both modes. Suburban particle size distributions exhibited notable seasonal disparities with differing influence of local formation, particularly in spring and summer, and transport which dominated in the fall season leading to notably higher sulfate and organic accumulation mode particle concentrations. Variations in particle mixing state were evaluated by comparison of inter-species mass median diameter trends at both measurement sites. Internal mixing was prevalent in the accumulation mode in spring at the urban site, while greater frequency of time periods with external mixing of particle populations comprising different fractions of organic constituents was observed in summer. At the suburban site, sulfate and nitrate in the accumulation mode more frequently exhibited differing particle size distributions in all seasons signifying a greater extent of external mixing.

At the urban site, periods of greater submicron inorganic mass concentrations were more likely to be caused by increases in both Aitken and accumulation mode particle mass in summer, while at the suburban receptor location organic and nitrate Aitken mode particle mass contributed more regularly to higher total submicron species mass concentrations in most seasons (spring, summer and winter).

30 1. Introduction

31 Apart from mass and chemical composition, the size distribution of fine particles represents a vital physical property
32 with important implications for human health and environmental effects of ambient aerosols (Seinfeld and Pandis,
33 2006). Particle size relates directly to the aerodynamic properties which govern the penetration and deposition of
34 particles in the airways and lungs (Davidson et al., 2005) as well as the scattering and absorption of light which affect
35 the radiative properties and hence ambient visibility (Ahlquist and Charlson, 1967;Bohren and Huffman,
36 1983;Charlson et al., 1991;Schwartz, 1996;Seinfeld and Pandis, 2006). Hygroscopic growth in response to changes in
37 ambient humidity can alter particle light scattering properties (Seinfeld and Pandis, 2006;Köhler, 1936) and activation
38 of condensation nuclei particles into cloud droplets depend on atmospheric conditions, chemical composition, mixing
39 state as well as the size and morphology of particles (Abbatt et al., 2005;Kerminen et al., 2012;Meng et al.,
40 2014;Westervelt et al., 2013).

41 Studies into the size distribution of ambient particulate matter in Hong Kong have been largely based on size-
42 segregated filter samples (Yao et al., 2007b;Zheng et al., 2008;Zhuang et al., 1999;Huang et al., 2014;Bian et al.,
43 2014) and measurements by electrostatic classifier instruments (Cheung et al., 2015;Yao et al., 2007a) and were hence
44 either limited in size resolution (offline filter samples) or chemical resolution (total particle count by classification).
45 Most measurements in Hong Kong were conducted in suburban environments. Inorganic ammonium and sulfate were
46 mainly found in fine mode particles in condensation and droplet mode size ranges, while nitrate had strong coarse
47 mode contributions (Zhuang et al., 1999). Seasonal differences were evident in solvent-extractable organics and trace
48 metals which were mainly found in PM_{0.5} particles in the wet season and winter whereas in fall a shift to larger particles
49 (0.5–2.5 µm fraction) in fall indicated a possibly stronger influence of aged particle components in the transition period
50 of the Asian monsoon (Zheng et al., 2008). Size distributions acquired by a fast mobility particle sizer at the suburban
51 HKUST supersite were investigated more recently to study the formation and accumulation of ultrafine particles under
52 different air flow regimes. Particle number concentration enhancements during the day were attributed to secondary
53 formation, while evening and nighttime peaks were thought to be related to transport of aged aerosols from upwind
54 locations. Nucleation mode particle peaks were often observed in fall and related to regional pollution influence
55 (Cheung et al., 2015). New particle formation events at the same site occurred as single and two-stage growth
56 processes with organics and sulfuric acid contributing mainly to first stage growth in the daytime while nighttime
57 second stage growth was attributed to ammonium nitrate and organics. Particle size growth into the diameter range of
58 cloud condensation nuclei (CCN) was typically only achieved with the second growth stage (Man et al., 2015).

59 Investigations into particle size distributions in urban areas of Hong Kong are even scarcer. Yao et al. (Yao et al.,
60 2007a) studied the properties and behavior of particles in vehicle plumes and reported a competing process between
61 ambient background particles and fresh soot particles in the condensation of gaseous precursors and a dependency on
62 temperature with bimodal volume size distributions observed at lower ambient temperatures and unimodal
63 distributions in the lower accumulation size range at higher ambient temperatures.

64 The Aerodyne aerosol mass spectrometer (Canagaratna et al., 2007) is widely used to determine the chemical
65 composition of major organic and inorganic components of non-refractory submicron particulate matter (NR-PM₁).
66 In contrast to most traditional aerosol sizing instruments, the AMS is capable of resolving main chemical constituents

67 within size distributions through analysis of particle flight times and particle ensemble mass spectra (Canagaratna et
68 al., 2007;Jayne et al., 2000;Jimenez et al., 2003;Rupakheti et al., 2005) and thus yields valuable additional information
69 on differences in composition of submicron particles with the gross of particle mass in the Aitken mode range ($D_p \sim$
70 10-100nm) and the accumulation mode range ($D_p \sim 100-1000\text{nm}$) covered by the AMS. Thus far most studies
71 employing ambient size distribution data from aerosol mass spectrometer measurements investigated longer time
72 period averages, i.e. campaign averages (Salcedo et al., 2006;Sun et al., 2009;Aiken et al., 2009;Huang et al.,
73 2010;Takegawa et al., 2009;Saarikoski et al., 2012;Li et al., 2015) or specific time periods of interest (Elser et al.,
74 2016;Lee et al., 2013). Mohr et al. separated organic particle mass size distributions by periods of dominant influence
75 of different PMF-resolved organic aerosol factors to study the properties of mass size distributions in relation to
76 organic aerosol composition (Mohr et al., 2012). The 3D-factorization technique is an extension of traditional AMS
77 PMF analysis on organic aerosol allowing to obtain estimates on the size distributions of organic aerosol factors,
78 however under the assumption that factor size distributions remain invariant over the measurement period (Ulbrich et
79 al., 2012).

80 The temporal evolution of species-specific size distributions, are mostly discussed qualitatively (Drewnick et al.,
81 2005) and only few studies have evaluated temporal trends in mass size distributions in greater detail.
82 Particle nucleation and subsequent growth events were investigated in Pittsburgh using size data from an AMS and
83 two SMPS as well as various gaseous pollutant instruments and meteorological information. The AMS mass size
84 distributions were evaluated quantitatively using the time series of binned particle concentrations generated from the
85 grouping of raw data into wider size bins to represent different stages in the particle growth process. (Zhang et al.,
86 2004). The same method was employed to evaluate contributions of ultrafine mode and accumulation mode particles
87 to total organic particle mass (Zhang et al., 2005) by summation of size bins in the range of 30-100 nm and 100-
88 1000nm. The authors also explored diurnal changes in size distributions of particle species by averaging over 3h
89 periods in the morning (6–9 am) and afternoon (1–4 pm). Sun et al. present a qualitative discussion of diurnal
90 variations in the mass size distributions of the m/z 44, m/z 57 and derived C_4H_9^+ ion signals from measurements at an
91 urban site in New York (Sun et al., 2011). Similarly, Setyan et al. examined diurnal changes in the mass size
92 distributions of organics and sulfate qualitatively and used binned concentrations (40–120, 120–200, and 200–800)
93 nm in their quantitative analysis to study the evolution of particle chemistry in new particle formation and growth
94 events (Setyan et al., 2012).

95 In this work, we introduce a systematic approach of analyzing AMS mass-based particle size distributions on finer
96 time scales and thus utilize two key instrumental advantages, i.e. species segregation and high time resolution, to
97 obtain a more detailed understanding of the variabilities in ambient particle mass size distributions and to provide an
98 additional dimension to standard AMS data analysis techniques. In this context, we present a detailed discussion of
99 particle size data from HR-ToF-AMS measurements during two field campaigns in Hong Kong in both urban and
100 suburban environments. We aim to evaluate characteristic recurrent changes in size distribution as well as longer term
101 trends in different seasons by analyzing day-to-day variations and diurnal variations of size distributions of submicron
102 organics, sulfate, and nitrate particle mass. The two contrasting sites represent a typical urban source environment
103 (inner-city, roadside station) close to primary emission sources and a suburban location (coastal, HKUST supersite)

104 which is largely a downwind receptor of varying amounts of local urban, regional and long-range transported
105 pollutants (Li et al., 2015;Huang et al., 2014).
106

107 **2. Methodology**

108 **2.1. Field campaigns**

109 Sampling of ambient submicron non-refractory particulate matter (NR-PM₁) was carried out using an Aerodyne HR-
110 ToF-AMS at the HKUST air quality supersite covering four seasons between May 2011 and February 2012 (spring:
111 2011-05, summer: 2011-09, fall: 2011-11&12, winter: 2012-02). The HKUST supersite is located on the campus of
112 the Hong Kong University of Science and Technology (22°20'N, 114°16'E), on the east coast of Hong Kong in a
113 suburban area with few primary emission sources in the immediate vicinity. Sampled air was drawn from the rooftop
114 of a pump house building at an approximate height of 25m above ground level. For detailed descriptions of the
115 experimental setup, operating conditions, data treatment, and overall species composition we refer the reader to
116 previous publications (Lee et al., 2013;Li et al., 2015;Li et al., 2013). A further sampling campaign took place between
117 spring 2013 (2013-03 to 2013-05) and summer 2013 (2013-05 to 2013-07) at an inner-city urban location in the
118 densely populated and built-up Kowloon peninsula. Measurements were conducted next to the roadside air quality
119 monitoring station (AQMS) operated by the Environmental Protection Department (EPD) of the HKSAR Government
120 in the Mong Kok (MK) district on a pedestrian crossing at a major road junction. Sampled air was drawn from a height
121 of 3m above ground level. A comprehensive analysis of trends in species concentration and composition identified in
122 this urban campaign has been presented previously (Lee et al., 2015). In both campaigns, particles were sampled
123 through a PM_{2.5} cyclone at a flow rate of 16.67 L/min into a sampling port from which 0.08 L/min was drawn by the
124 AMS and the remainder drawn by co-sampling instruments and an auxiliary pump. Sample air for the AMS passed
125 through a 1m long diffusion dryer (BMI, San Francisco CA, USA) filled with silica gel to remove bulk gas- and
126 particle-phase water. Additional data from various collocated instruments including meteorological data (wind,
127 temperature, relative humidity, solar irradiation), volatile organic compounds (VOCs) and standard trace gases such
128 as NO_x, SO₂, and O₃ were available and details on employed instrument models and sampling methodologies are
129 discussed in aforementioned studies (Lee et al., 2013, 2015;Li et al., 2015;Li et al., 2013).

130 **2.2. Data acquisition and treatment**

131 In both campaigns, mass concentration based size distributions in terms of vacuum-aerodynamic particle diameter
132 ($dM/d\log D_{va}$) were established by joint acquisition of particle time-of-flight (PToF) measurements and unit mass
133 resolution mass spectra (V-mode) with alternation between modes every 20s for 30 cycles amounting to 5 min of total
134 sampling time. High-resolution mass spectra were acquired for the following 5 min, and thus the overall raw data time
135 resolution for each mode was equal to 10 min. The total particle mass measured in the PToF mode was normalized to
136 the V-mode mass concentration of the same time step. Daily size distributions were generated by averaging over 24h

137 periods (from 0:00 to 23:59). Hourly diurnal size distributions were reconstructed by grouping size distributions within
138 the same hour of the day and establishing representative size distributions based on average, median, 25th and 75th
139 percentile concentration values of each size bin (*referred to as size distribution sets hereinafter*).

140 At both sampling sites, the seasonally averaged AMS size distributions were bimodal (Lee et al., 2013, 2015; Li et al.,
141 2015) with similar distributions having been observed in other AMS field studies in various parts of the world. (Zhang
142 et al., 2014; Sun et al., 2011; Huang et al., 2011; Aiken et al., 2009; Zhang et al., 2005; Crippa et al., 2013; Docherty et
143 al., 2011; Mohr et al., 2012). Multimodality of size distributions is typical for environments where different sources or
144 formation processes of particles play a role and accordingly such distributions can also be represented as sums of
145 discrete lognormal distributions of the respective constituting submodes (John, 2011).

146 The measured bimodal size distributions in this work were deconvoluted by fitting two log-normal distributed modes,
147 including one closer to the Aitken size range (*mode diameter ~100nm*) and one in the accumulation size range (*mode*
148 *diameter ~500nm*) employing the Levenberg-Marquardt algorithm (Gill et al., 1981) as a non-linear least squares fit,
149 to evaluate differences in trends and formation or transformation processes in the two size regimes. An example of a
150 size distribution fit and associated parameters is depicted in Figure D1 in the Supporting Material. Additional fit
151 residual analyses were carried out in cases where the Aitken mode only accounted for small parts of (<10%) of the
152 total particle mass and uncertainties in integrated mode particle mass from the peak fitting were examined for all size
153 distributions. Details are presented in Section B of the Supporting Material. The smaller mode typically exhibited
154 mode diameters in the range of 100-200 nm (D_{va}) and is thus in the transition region between Aitken and lower
155 accumulation mode. For a clearer distinction from the larger mode which unambiguously belonged to the
156 accumulation size range, we opt to refer to the small mode as *Aitken mode* in this work. Mode diameter (*i.e.* mass
157 median diameter, MMD), curve width (*i.e.* geometric standard deviation, GSD) and curve area (*equivalent to particle*
158 *mass concentration within the mode*) are sufficient parameters to completely describe a lognormal distribution and
159 these key variables are used in the following analysis on trends in the fitted species-specific size distributions of
160 organics, nitrate, and sulfate from both HR-AMS sampling campaigns in Hong Kong. Particle diameters are discussed
161 in terms of vacuum-aerodynamic diameter, with detailed discussions on properties and relationships to other size
162 metrics available elsewhere (DeCarlo et al., 2004; Slowik et al., 2004). Further details on procedures of PToF data
163 acquisition and size distribution averaging can be found in the Supporting Material in Section A and B respectively.
164 The sequence of main data treatment and analysis steps is shown in Figure 1.

165 The transmission efficiency of the AMS aerodynamic lens is known to fall off beyond ~0.7 μm of vacuum-
166 aerodynamic diameter (Liu et al., 2007; Takegawa et al., 2009; Zhang et al., 2004; Bahreini et al., 2008; Williams et al.,
167 2013) and may bias measured particle mass and mode diameters in the accumulation mode towards lower values if
168 significant particle mass fractions fall in the size region of $D_{va} > 0.7 \mu\text{m}$. In this work, resolved MMDs at either
169 sampling location were well within the efficient upper transmission limit for the vast majority of data.

170 The discussion of size distributions in this work should be viewed in the context of the instrumental capabilities and
171 limitations of aerosol mass spectrometry, *i.e.* resolved Aitken and accumulation modes in this work are the apparent
172 Aitken and accumulation modes within AMS measurable particle mass size distributions.

173

368 **Figure 3.** Diurnal variations of mode diameter (MMD), integrated mode mass concentration and width of the Aitken mode (*lighter*
369 *color*) and accumulation mode (*darker color*) from bimodal peak fits of the bin-median reconstructed size distributions at the
370 suburban HKUST site and V-mode AMS species concentrations (line with shaded background) for organics, nitrate and sulfate
371 (left to right) in (a) Spring 2011, (b) Summer 2011, (c) Fall 2011 and (d) Winter 2012; The right-most panel depicts the diurnal
372 variations of relevant gas-phase pollutants (O₃, CO, NO_x, SO₂) measured at the same site.
373

374
375 **Figure 4.** Diurnal variation of the fraction of Aitken mode particle mass among total submicron species mass for organics (*top*),
376 nitrate (*middle*) and sulfate (*bottom*) at the (a) urban Mong Kong site, and (b) suburban HKUST supersite in different seasons;
377 *based on concentrations from bin-median size distributions, seasons denoted by marker color and type of marker symbol*

378 3.1.2. Suburban coastal NR-PM₁

379 The suburban HKUST site as a downwind receptor of urban and regional pollution was generally dominated by sulfate
380 and oxygenated secondary organic aerosol (SOA) components and much lower fractions of primary organic
381 constituents, which combined typically made up less than a quarter of total organics (Li et al., 2015).

382 383 Organics

384 There were significant seasonal differences with larger fractions (Figure 4a) and concentrations (Figure 5c) of Aitken
385 mode mass in total organic submicron particle mass in spring and summer compared to fall and winter, indicating
386 greater influence of closer-ranged formation sources in the warmer season. Springtime integrated Aitken mode mass
387 concentrations ($\sim 0.8 \mu\text{g}/\text{m}^3$) were twice as high as those in winter ($\sim 0.4 \mu\text{g}/\text{m}^3$). In the accumulation mode, highest
388 particle mass loadings were observed in fall ($5 \mu\text{g}/\text{m}^3$) and lowest loadings in spring ($3 \mu\text{g}/\text{m}^3$) following the frequency
389 pattern of continental air mass influence (Figure D12 in the Supporting Material) in each season indicating continental

390 transport of particulate mass or gas-phase precursors. Lowest mass concentrations in the Aitken mode typically
391 occurred in the night hours (00:00 – 05:00) in a range of 0.3 – 0.5 $\mu\text{g}/\text{m}^3$ in spring, summer, and winter, while in fall
392 mass loadings of 0.7 - 0.8 $\mu\text{g}/\text{m}^3$ were reached. Diurnal changes were least pronounced in winter with largely constant
393 integrated Aitken mode particle concentrations. In the remaining seasons, varying degrees of daytime changes were
394 apparent with a general increase around 06:00, likely owing to citybound commuter traffic from surrounding roads to
395 the west of the sampling site at 1-2km of lateral distance. This also led to a modest increase in particle polydispersity
396 with a discernible widening of the Aitken mode size distributions (*black solid line, lowest panels in Figure 3*). Daily
397 maxima in spring, summer and fall were reached in the early evening (~21:00) with marked differences in absolute
398 mass concentrations depending on the respective season, from a summer time low of 0.8 $\mu\text{g}/\text{m}^3$ to a fall season high
399 of 1.4 $\mu\text{g}/\text{m}^3$. Mass median diameters in the Aitken mode were smaller in the night hours and displayed subtle
400 increments during the day in the range of 10-20 nm reaching their maximum typically in the late afternoon, except for
401 the fall season when mass median diameters displayed very little variation with time of day.

402 Total particle mass in the accumulation mode in spring and summer reached minima during the night hours (2 $\mu\text{g}/\text{m}^3$)
403 and maxima (3 $\mu\text{g}/\text{m}^3$) around noon, remaining stable in the daylight hours thereafter. MMDs increased notably from
404 440nm at night to 510nm during the day in spring, while in summer a morning rise by ~30nm from 530nm to 560nm
405 was obvious between 06:00 and 10:00 and coincided with the morning rush hour and the associated early morning
406 peak of NO_x and an otherwise stable mode diameter of 530nm for the rest of the day. In fall, the increase in
407 accumulation mode organic mass occurred much earlier, starting in the dark hours at 04:00, with a corresponding
408 trend also evident for nitrate but absent for sulfate, indicating a common source of these organic and nitrate enriched
409 particles. Nighttime MMDs for organics were generally larger (540nm) and decreased to a minimum of 510nm in the
410 early afternoon accompanied by a slight widening of the distribution. In winter, mass concentrations decreased
411 appreciably in the early morning hours and started to increase only beyond 10:00. In the colder seasons (fall, winter),
412 a similar concentration pattern was also observed for gas-phase SO_2 which is considered as a largely regional pollutant
413 with few distinct local sources (Yuan et al., 2013), indicating that changes in boundary layer and mixing with regional
414 background were likely the more dominant processes in winter.

415

416 Sulfate

417 Aitken mode sulfate mass concentrations peaked in the afternoon from spring throughout fall with maximum
418 concentrations reached progressively later in the afternoon (14:00 in spring; 16:00 in fall). Nominal concentrations
419 were highest in spring and summer (0.5-0.6 $\mu\text{g}/\text{m}^3$), slightly lower in fall (0.4 $\mu\text{g}/\text{m}^3$) and reached the lowest levels in
420 winter (0.1 $\mu\text{g}/\text{m}^3$). In addition to the afternoon peak, a conspicuous early morning peak of similar magnitude was
421 evident in spring between 02:00 and 06:00. A greater proportion of southerly winds was evident in said time period
422 compared to the overall seasonal wind frequency distribution (Figure D13a in the Supporting Material) and may
423 indicate transport of sulfate from marine sources in the southern parts of Hong Kong. Diurnal variations in MMDs
424 and GSDs were generally small and without obvious regular trends. Nominal mass median diameters were
425 significantly lower in winter (~170nm) compared to spring and fall (~190nm) and summer (~210nm).

426 Trends in accumulation mode particle mass were more pronounced. In spring, a shallow concentration valley during
427 the late evening and night hours (20:00 to 03:00) with minimum concentrations of $5 \mu\text{g}/\text{m}^3$ was apparent, while
428 daytime concentrations stayed largely invariant at $6 \mu\text{g}/\text{m}^3$. The MMDs followed a similar variation with a minimum
429 mode diameter around 550nm in the early hours of the day and slightly larger daytime MMDs around 570nm. Nominal
430 concentrations were larger in summer with a nighttime valley concentration of $7 \mu\text{g}/\text{m}^3$ and a well-pronounced broad
431 day peak with a maximum of $9.5 \mu\text{g}/\text{m}^3$ in the early afternoon (14:00-15:00). A prior additional morning peak occurred
432 between 04:00 and 10:00 with particle mass concentrations reaching $8.5 \mu\text{g}/\text{m}^3$ related to a consistent north-easterly
433 morning wind pattern (Figure D13b in the Supporting Material) and likely associated with transport from north-
434 easterly coastal regions or nighttime fisheries related maritime traffic. The diurnal trend in mass median diameter was
435 similar to that in spring with a night minimum of 570nm and day maximum of 590nm.

436 In fall, accumulation mode characteristics showed no significant diurnal variability, with a largely stable integrated
437 particle mass of $6 \mu\text{g}/\text{m}^3$ and only subtle MMD changes (585nm at night; 575nm during the day). In winter, two
438 concentration dips with reductions by $\sim 0.5 \mu\text{g}/\text{m}^3$ between 06:00 and 10:00 and between 18:00 and 22:00 were evident,
439 while MMDs increased during the day between 10:00 and 15:00 from 520nm, peaking at a size of 540nm.

440

441 Nitrate

442 Nitrate particle mass in the Aitken mode was generally small from spring throughout fall amounting to 0.01 - 0.06
443 $\mu\text{g}/\text{m}^3$. Winter time concentrations were larger in a range of 0.06 - 0.08 $\mu\text{g}/\text{m}^3$ during the day and 0.10 - 0.12 $\mu\text{g}/\text{m}^3$ in
444 the late evening hours. The latter evening peak centered around 21:00 was evident in most seasons (except spring)
445 and accounted for 12-23% (0.1-0.25 $\mu\text{g}/\text{m}^3$) of total daily Aitken mode nitrate mass burden. Similar to the urban
446 roadside location, these nighttime nitrate peaks coincided with the peak period of organic cooking aerosol
447 concentrations (Figure D14 in the Supporting Material), which were however significantly smaller at the suburban
448 measurement site and mainly attributed to the operation of an on-campus student canteen (Li et al., 2015). Trends in
449 mass median diameters varied between seasons with no discernible trend in winter, a subtle decreasing trend with time
450 of day in spring and broad daytime diameter increases in summer and fall. Solar irradiation in these two seasons was
451 comparatively high (Figure D10b,c in the Supporting Material) indicating that photochemical nitrate production in the
452 Aitken mode may have led to this observed growth in particle size.

453 Integrated particle mass concentrations in the accumulation mode only exhibited subtle variations from spring
454 throughout fall, with essentially constant diurnal concentrations in spring, a subtle daytime peak in summer which
455 accounted for $\sim 15\%$ of total daily accumulation mode nitrate (corresponding to $0.7 \mu\text{g}/\text{m}^3$) and a conspicuous morning
456 peak between 04:00 and 10:00 in fall accounting for $\sim 5\%$ of total daily accumulation mode nitrate (corresponding to
457 $0.5 \mu\text{g}/\text{m}^3$). Clearer seasonal differences were evident in the trends of MMDs. In spring, MMDs decreased appreciably
458 over the late evening hours (21:00-0:00) with a concurrent widening of the size distribution (increase in GSD). In
459 summer, accumulation mode diameters decreased during the day by $\sim 40\text{nm}$ with a similar trend in accumulation mode
460 organics. Winter time MMDs exhibited a more complex pattern with larger mode diameters in the early hours (04:00
461 – 10:00) and during the noon-time, and a late-afternoon dip leading to larger spread of intra-day mode diameters
462 ranging from 510nm to 570nm.

463 In comparison to the urban roadside measurements, diurnal particle size characteristics and mass concentrations in the
464 Aitken and accumulation mode were much more variable for all investigated species at the suburban HKUST site,
465 indicating that longer time scale processes and irregular events (transport patterns, local meteorology) were probably
466 more important in governing particle size distribution characteristics than diurnal processes.

467 **3.2. Day-to-day size distributions**

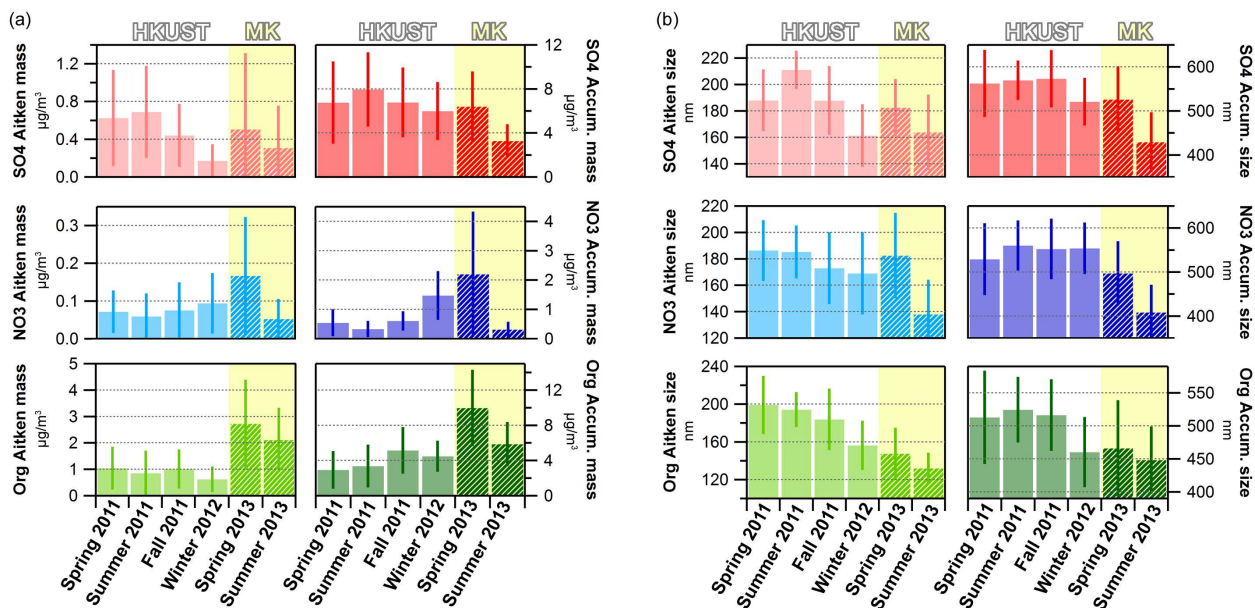
468 To evaluate the evolution of particle size distributions within seasons, average species-specific size distributions were
469 generated by averaging raw distributions over 24h periods (between 0:00 and 23:59). There was clear long-term
470 variability in both resolved Aitken and accumulation mode MMDs and integrated submode particle mass
471 concentrations for all species (Figure D15 in the Supporting Material) and overall seasonal differences which have
472 been briefly addressed in the discussion of the diurnal size distribution variations between seasons. Figure 5 depicts
473 the overall average values for all daily fitted MMDs and integrated particle mass concentrations in both the Aitken
474 and accumulation mode at the suburban HKUST and urban MK sites.

475 **3.2.1. Seasonal trends**

476 For the MK roadside station, particle mode diameters were generally larger in spring than in summer for all three
477 investigated species, but with clear differences in the magnitude of changes among individual species. In the Aitken
478 mode, organics and sulfate displayed a moderate decrease in mode diameter by 7-8% each, while nitrate saw a more
479 significant decrease by 25% from spring to summer. In contrast, accumulation mode MMDs for organics exhibited
480 only a subtle decrease by 5% and more substantial decreases for sulfate and nitrate by 20-22% each. Total Aitken
481 mode particle mass decreases varied strongly: -15% for organics, -36% for sulfate and -67% for nitrate. In the
482 accumulation mode, organics and sulfate exhibited similar relative decreases by 40-46%, while nitrate particle mass
483 reduced drastically by 85%.

484 At the suburban HKUST site, Aitken mode MMDs of nitrate and organics decreased with the progression of seasons
485 from spring to winter with highest mode diameters observed in spring and summer and appreciable decreases in winter
486 by -9% for nitrate and -25% for organics compared to the warmer seasons. Sulfate displayed a similar winter time
487 decrease in MMD (-15%) and an increase of similar magnitude in the summer season (+13%) compared to spring and
488 fall. Variations in sulfate and organic accumulation mode diameters were minor between spring and fall, while
489 wintertime MMDs were 7-12% lower. Nitrate exhibited an overall higher variability in mass median diameters in the
490 accumulation mode in spring (larger standard deviation) and with on average 10% lower MMDs compared to other
491 seasons. In line with the reduction in Aitken mode MMDs in winter, the integrated Aitken mode particle mass
492 decreased as well, by -16% for organics and almost -75% for sulfate, whereas nitrate contributions remained largely
493 stable throughout the seasons. Organic accumulation mode particle mass was significantly higher in the fall and winter
494 season by factors of 1.6 – 2. Diurnal variations in the degree of oxygenation were least pronounced in these seasons
495 (Li et al., 2015) suggesting that influence of transport in autumn and winter likely dominated over local formation,

496 thus exerting greater effects on particle mass in the larger size mode. Particulate nitrate concentrations were generally
 497 low in the accumulation mode from spring through fall, but increased sharply in winter by factors of 3 – 4. Sulfate
 498 accumulation mode mass concentrations remained more stable but saw significant summer time enhancements by
 499 ~30% likely due to photochemical activity which also led to high concentrations of Ox and a higher degree of
 500 oxygenation of organic aerosol among the four seasons (Li et al., 2015).
 501



502
 503 **Figure 5.** Average and standard deviation of daily fit values of Aitken and accumulation mode particle mass and mass median
 504 diameters at the suburban HKUST site (*solid bars*) and urban MK site (*hashed bars*). The integrated particle mass is depicted in
 505 (a), (b), (c) for the Aitken mode, and in (d), (e), (f) for the accumulation mode for sulfate, nitrate, and organics respectively. The
 506 mass median diameter is depicted in (g), (h), (i) for the Aitken mode and in (j), (k), (l) for the accumulation mode for sulfate,
 507 nitrate and organics respectively.

508
 509 Large particles contribute more to particle volume and hence particle mass. Correspondingly, the total submicron
 510 concentration of a given species is typically governed by changes in the accumulation mode particle mass and
 511 accordingly observed correlation values between integrated accumulation mode particle mass and individual NR-PM₁
 512 species mass concentrations were generally high ($R_{pr} > 0.90$) at both measurement sites (Figure D16 in the Supporting
 513 Material). This applied to both measurement sites regardless of the season. Aitken mode trends were less akin. At the
 514 urban roadside station, neither sulfate nor nitrate particle mass in the Aitken mode notably correlated with the
 515 respective total submicron species mass concentration in spring (all $R_{pr} \leq 0.20$), whereas in summer correlations were
 516 more significant with $R_{pr} = 0.51$ for sulfate and $R_{pr} = 0.80$ for nitrate. This signifies that periods of greater species mass
 517 concentrations were more likely to be caused by increases in both Aitken and accumulation mode particle mass
 518 indicating that particle formation and growth affecting smaller particles was more likely to occur in the warmer season.
 519 For organics, Aitken mode particle mass and submicron species mass correlated only weakly ($R_{pr} = 0.26$ in spring and

520 $R_{pr} = 0.38$ in summer), i.e. each organic particle submode was governed by largely different dominant sources or
521 formation processes in both seasons at the roadside.

522 At the suburban background site, Aitken mode particle mass for sulfate showed little correlation with total submicron
523 sulfate concentration ($R_{pr} \leq 0.10$) apart from the spring season ($R_{pr} = 0.36$) where more frequent wet and foggy
524 conditions may have facilitated sulfate formation in both size modes. For organics and nitrate significantly larger
525 correlation coefficients of submode particle mass to total species concentration ($0.5 \leq R_{pr} \leq 0.7$) were observed in
526 most seasons (spring, summer, winter) indicating significant influence of local or regional formation processes on
527 organic and nitrate Aitken mode particulate mass at the suburban receptor location. In the fall season, much weaker
528 correlations ($0.2 \leq R_{pr} \leq 0.4$) were likely caused by the dominance of continental air mass influence (Figure D12c in
529 the Supporting Material) and greater influence of aged accumulation mode particles on total submicron nitrate mass
530 concentrations.

531 **3.2.2. Inferred changes in mixing state**

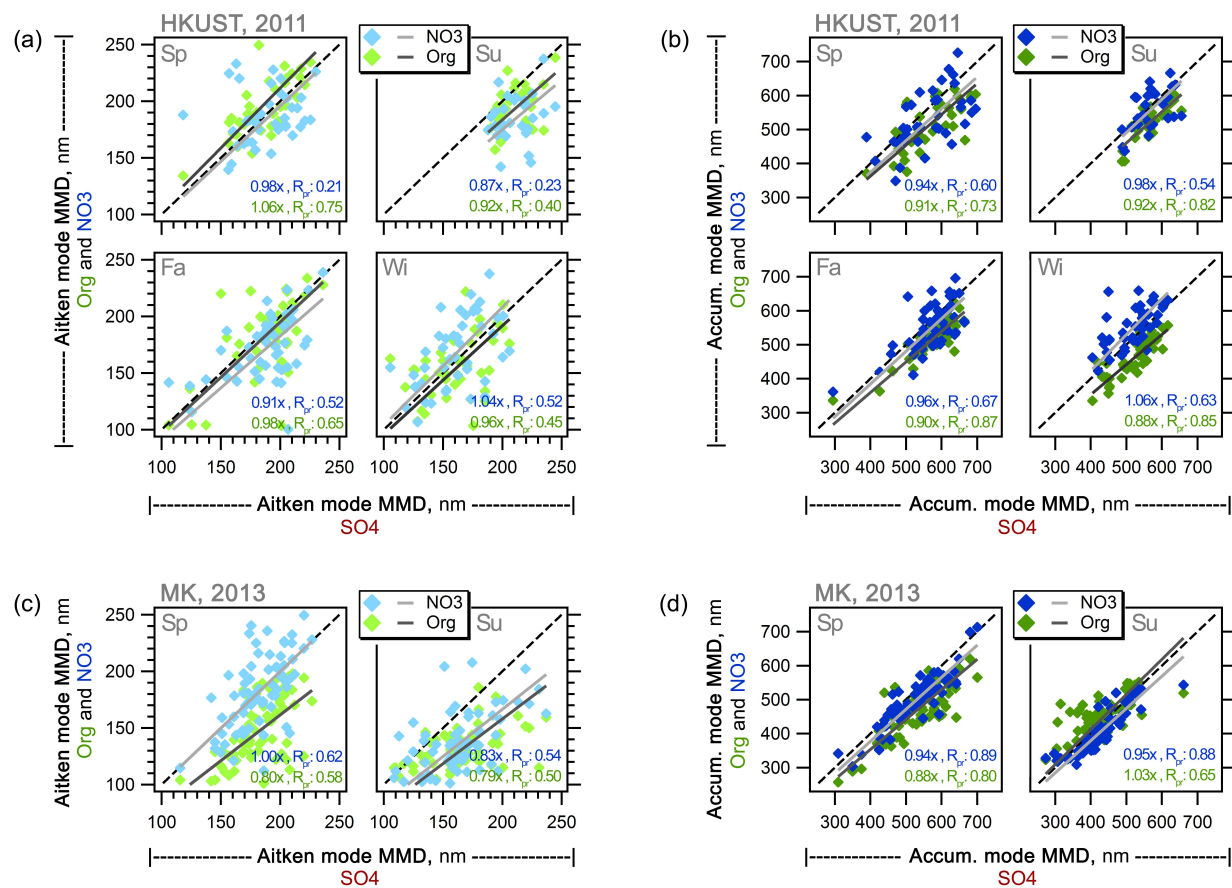
532 Shifts in mixing state of ambient particles can be inferred from the inter-species analysis of mass median diameters.
533 Close nominal agreement (i.e. diameter ratios close to 1) infer that different species were distributed similarly across
534 the particle size range which thus most likely represents a largely internally mixed particle population, while the spread
535 of data (correlation coefficient) indicates the temporal homogeneity or divergence of resolved mode diameters. A
536 hypothetically perfectly internally mixed particle population over the whole sampling period would, therefore, yield
537 MMD ratios and Pearson's R values of 1 between species, while larger or smaller values are indicative of a greater
538 frequency of heterogeneous (i.e. more externally mixed) particle populations (Figure 6).

539 At the urban Mong Kok site, changes in accumulation mode mass median diameters for nitrate and sulfate followed
540 similar trends ($R_{pr} = 0.88-0.89$) and with diameter ratios close to 1 (0.94–0.95) Similarly, fitted accumulation mode
541 diameters of organic constituents predominantly followed that of sulfate in spring nominally (diameter ratio 0.88) and
542 temporally ($R_{pr} = 0.80$). The nominal agreement of organic and sulfate accumulation mode diameters persisted
543 (diameter ratio 1.03) overall in summer, however, there was significantly more temporal divergence ($R_{pr} = 0.65$)
544 indicating a greater frequency of time periods with external mixing of particle populations comprising different
545 fractions of organic constituents.

546 External mixing is more prevalent for freshly formed smaller particles which have typically undergone less
547 condensational growth, coagulation or aqueous-phase reactions. Indeed, the correlation coefficients of both nitrate
548 and organic Aitken mode MMDs with respect to sulfate were notably lower (0.50 and 0.62) indicating frequent periods
549 of particle populations with different species prevailing in different size regions within the Aitken mode.

550 Sulfate and nitrate were still more likely to occur internally mixed in the Aitken mode in spring with similar diameters
551 (nitrate to sulfate MMD ratio = 1.00), while organic Aitken mode MMDs were consistently lower, indicating greater
552 fractions of organic dominated particles towards the lower end and more inorganic dominated particles towards the
553 upper end of the fitted Aitken mode.

554 In summer, both nitrate and organic MMDs tended to be lower than those of sulfate (diameter ratios of 0.79 – 0.83)
555 but similar to each other, thus implying a shift to externally mixed populations of more nitrate and organic enhanced
556 and internally mixed smaller Aitken mode particles and sulfate dominated larger Aitken mode particles.
557 At the suburban HKUST site, accumulation mode MMDs of both nitrate and organics were generally quite similar to
558 those of sulfate with diameter ratios of 0.88 – 1.06. Compared to the urban site, correlation coefficients of nitrate and
559 sulfate were consistently lower (0.54 – 0.67) indicating a much greater frequency of time periods where sulfate and
560 nitrate dominated particles in the accumulation exhibited significantly different particle size distributions.
561 In winter, organic MMDs were consistently lower than those of sulfate and nitrate indicating a greater proportion of
562 externally mixed particle populations with organics enriched particles in the lower accumulation size range and
563 inorganic dominated particles in the larger accumulation size range. The least variability in particle size was observed
564 in the summer season where MMDs in both Aitken and accumulation mode displayed variations in relatively narrow
565 ranges between 200-250nm and 500-700nm, whereas in the remaining seasons time periods with particle populations
566 of lower MMD were more frequent, extending to MMDs as low as 100nm in the Aitken mode and 300nm in the
567 accumulation mode.
568 In the Aitken mode, mass median diameters overall were quite similar across species, with diameter ratios of organic
569 and nitrate distributions to those of sulfate in the range of 0.87 – 1.06, indicating that they generally covered a similar
570 size range. The temporal agreement was highly variable with correlation coefficients (R_{pr}) spanning from 0.21 to 0.75
571 indicating that Aitken mode particle populations at the suburban site were generally more diverse and likely influenced
572 by a greater range of particle formation and growth mechanisms compared to the urban Mong Kok site.
573



574
 575 **Figure 6.** Scatter plots of fitted mass median diameters of organics and nitrate vs. sulfate for the (a) Aitken mode and (b)
 576 accumulation mode at the urban Mong Kok site, and (c) Aitken mode and (d) accumulation mode at the HKUST suburban site
 577

578 **3.3. Comparison to previous studies**

579 Particle size distribution studies in Hong Kong are generally scarce and have focused on either size segregated filter
 580 samples (MOUDI) for general ambient measurements or electrostatic classification in particle formation and particle
 581 growth studies (Guo et al., 2012; Cheung et al., 2015). The latter studies focus on specific and narrow time periods
 582 and lack general discussions on ambient particle size distributions.

583 Two ambient studies were undertaken at the suburban coastal HKUST site using size-segregated samples from a ten-
 584 stage MOUDI sampler and offline chromatographic analysis. Inorganic constituents (NH₄, NO₃, SO₄) in fine particles
 585 (i.e. D_p < 1.8 μm) were shown to follow bimodal distributions with mode diameters in the range of 0.14-0.21 μm and
 586 0.46-0.58 μm in samples collected in the winter season, while the main mode was observed in the coarse region (4-6
 587 μm) for all three species (Zhuang et al., 1999). A subsequent year-long observational study also reported bimodal fine
 588 particle distributions with mode diameters of 0.1-0.3 μm and 0.7-0.9 μm and 1-2 additional modes in the coarse region
 589 (Bian et al., 2014), however, the main mode in the size distributions of sulfate, ammonium, potassium and oxalate
 590 was observed in the droplet mode (0.7 - 0.9 μm) in this study. Vehicle exhaust plumes sampled on-road from a Mobile

591 Real-time Air Monitoring Platform (MAP) across Hong Kong's road network exhibited three distinct particle volume
592 size distributions: a unimodal distribution with an accumulation mode at 0.2 μm and two bimodal distributions with a
593 minor mode at 0.2 μm and the dominant mode at 0.5 or 0.7 μm (Yao et al., 2007a).

594 The bimodality in the fine particle range across these studies is consistent with the AMS-based results in this work.
595 Nominally, the accumulation mode diameters from filter based studies and the chase studies are larger than those from
596 AMS measurements where maximum mode diameters occurred at $D_{va} \sim 700\text{nm}$, corresponding to $D_a \sim 470$ (assuming
597 $D_{va} \sim D_a * \text{density}$; particle density $\sim 1.5 \text{ g/cm}^3$). Direct comparability is however limited due to fundamental
598 differences in sizing techniques (MOUDI: atmospheric pressure; AMS: near-vacuum), sampling times (MOUDI: 24h
599 samples, scattered time line; AMS: minute raw resolution averaged to hourly or daily, continuous time line),
600 measurement uncertainties (MOUDI: sampling artifacts such as vapor adsorption and desorption; AMS: inlet lens
601 transmission) and aerosol pretreatment (none for MOUDI with potential impacts on particle size in high humidity
602 (>80%) conditions (Fang et al., 1991); AMS: removal of water prior to introduction to instrument).

603 4. Conclusion

604 A detailed analysis of AMS mass-based particle size distributions of sulfate, nitrate, and organics in submicron
605 particulate matter measured at two contrasting locations in Hong Kong during two field campaigns has been
606 undertaken. Deconvolution of size distributions into Aitken and accumulation submodes was accomplished by log-
607 normal peak fitting and trends in particle size (mass median diameters), dispersity (geometric standard deviation) and
608 overall particle mass (integrated mode area) were discussed on a diurnal time scale and on a daily basis to evaluate
609 longer-term changes in size distribution characteristics. At the urban roadside location, clear diurnal influences of
610 primary particle and gas-phase species were evident affecting both inorganic and organic component size distributions.
611 Traffic and cooking contributed an estimated 0.3 – 0.9 $\mu\text{g/m}^3$ and 0.5 – 1.8 $\mu\text{g/m}^3$ of organic component particle mass
612 in the Aitken mode, and 1.6 - 1.8 $\mu\text{g/m}^3$ and 1.0 – 2.7 $\mu\text{g/m}^3$ respectively in the accumulation mode with concentrations
613 level varying with seasons. Notable changes in Aitken mode mass median diameters of organics were limited to the
614 morning rush hour. Daytime particle concentration maxima of sulfate and nitrate in summer indicated substantial
615 influence of photochemical processes, which also led to increments in mass median diameters in the accumulation
616 mode thus inferring associated particle growth. Nocturnal nitrate formation was apparent in the accumulation mode
617 in spring concurring with the nighttime peak of ozone at the roadside, while in the Aitken mode nitrate particle
618 concentrations were significantly elevated during the dinner hours. Organics-related size distributions were mostly
619 governed by intra-day changes at the urban site with very similar trends across different size distribution sets (i.e.
620 concentration regimes), while disparities in diurnal variations among different size distribution sets were evident for
621 nitrate and sulfate, particularly affecting the average sets, indicating stronger influence of irregular external factors
622 which were not associated with diurnal time scale processes.

623 Suburban particle size distributions exhibited variable diurnal characteristics, suggesting that irregular processes such
624 as transport and seasonal meteorological conditions were the more dominant processes influencing particle size
625 characteristics. Aitken mode particle mass of organics was significantly larger in spring and summer indicating greater

626 influence of more local formation sources in the warm season. In the accumulation mode, organic particle mass
627 concentrations were highest in fall and lowest in spring, following the frequency pattern of continental air mass
628 influence. For sulfate, Aitken mode mass concentrations mass concentrations peaked in the afternoon from spring
629 throughout fall with highest nominal concentrations in spring and summer and lowest levels in winter, while
630 accumulation mode particle mass was highest in summer and fall and lowest in winter, similar to the trend observed
631 among organic constituents.

632 Nitrate particle mass in the Aitken mode was generally small in most seasons (0.01 - 0.06 $\mu\text{g}/\text{m}^3$), except winter where
633 daytime concentrations reached $\sim 0.1 \mu\text{g}/\text{m}^3$. In both modes, changes in mass median diameters varied temporally and
634 in magnitude with seasons, indicating a stronger influence of specific meteorological conditions on the properties of
635 nitrate-containing particles at the suburban site. At the urban site, periods of greater inorganic species mass
636 concentrations were more likely to be caused by increases in both Aitken and accumulation mode particle mass in
637 summer, indicating that particle formation and growth affecting smaller particles was more likely to occur in the
638 warmer season. At the suburban receptor location, significant correlation of submode particle mass to total species
639 concentration ($0.5 \leq R_{pr} \leq 0.7$) was observed for organics and nitrate in most seasons (spring, summer, winter)
640 suggesting notable influence of local or regional formation processes on organic and nitrate Aitken mode particulate
641 mass. Variations in particle mixing state were examined by evaluation of inter-species mass median diameter trends
642 at both measurement sites. In the accumulation mode at the urban site, internal mixing appeared to be prevalent in
643 spring, while greater frequency of time periods with external mixing of particle populations comprising different
644 fractions of organic constituents was observed in summer. External mixing was predominant in the Aitken mode at
645 the urban location in both seasons. At the suburban site, sulfate and nitrate in the accumulation mode more frequently
646 exhibited differing particle size distributions in all seasons signifying a greater extent of external mixing. In winter,
647 external mixing of more organics enriched particles in the lower accumulation size range was evident.

648 **Acknowledgements**

649 This work was supported by the Environmental Conservation Fund of Hong Kong (project number ECWW09EG04).
650 Chak K. Chan gratefully acknowledges the startup fund of the City University of Hong Kong.

651 **References**

- 652 Abbatt, J. P. D., Broekhuizen, K., and Pradeep Kumar, P.: Cloud condensation nucleus activity of
653 internally mixed ammonium sulfate/organic acid aerosol particles, *Atmospheric Environment*, 39,
654 4767-4778, 10.1016/j.atmosenv.2005.04.029, 2005.
- 655 Ahlquist, N. C., and Charlson, R. J.: A New Instrument for Evaluating the Visual Quality of Air, *Journal*
656 *of the Air Pollution Control Association*, 17, 467-469, 10.1080/00022470.1967.10469006, 1967.
- 657 Aiken, A. C., Salcedo, D., Cubison, M. J., Huffman, J. A., DeCarlo, P. F., Ulbrich, I. M., Docherty, K. S.,
658 Sueper, D., Kimmel, J. R., Worsnop, D. R., Trimborn, A., Northway, M., Stone, E. A., Schauer,

659 J. J., Volkamer, R. M., Fortner, E., de Foy, B., Wang, J., Laskin, A., Shutthanandan, V., Zheng,
660 J., Zhang, R., Gaffney, J., Marley, N. A., Paredes-Miranda, G., Arnott, W. P., Molina, L. T., Sosa,
661 G., and Jimenez, J. L.: Mexico City aerosol analysis during MILAGRO using high resolution
662 aerosol mass spectrometry at the urban supersite (T0) - Part 1: Fine particle composition and
663 organic source apportionment, *Atmospheric Chemistry and Physics*, 9, 6633-6653, 2009.

664 Bahreini, R., Dunlea, E. J., Matthew, B. M., Simons, C., Docherty, K. S., DeCarlo, P. F., Jimenez, J. L.,
665 Brock, C. A., and Middlebrook, A. M.: Design and Operation of a Pressure-Controlled Inlet for
666 Airborne Sampling with an Aerodynamic Aerosol Lens, *Aerosol Science and Technology*, 42,
667 465-471, 10.1080/02786820802178514, 2008.

668 Bian, Q., Huang, X. H. H., and Yu, J. Z.: One-year observations of size distribution characteristics of
669 major aerosol constituents at a coastal receptor site in Hong Kong – Part 1: Inorganic ions
670 and oxalate, *Atmos. Chem. Phys.*, 14, 9013-9027, 10.5194/acp-14-9013-2014, 2014.

671 Bohren, C. F., and Huffman, D. R.: Absorption and scattering of light by small particles, in: *Absorption*
672 *and Scattering of Light by Small Particles*, Wiley-VCH Verlag GmbH, 1-11, 1983.

673 Canagaratna, M. R., Jayne, J. T., Jimenez, J. L., Allan, J. D., Alfarra, M. R., Zhang, Q., Onasch, T. B.,
674 Drewnick, F., Coe, H., Middlebrook, A., Delia, A., Williams, L. R., Trimborn, A. M., Northway,
675 M. J., DeCarlo, P. F., Kolb, C. E., Davidovits, P., and Worsnop, D. R.: Chemical and
676 microphysical characterization of ambient aerosols with the aerodyne aerosol mass spectrometer,
677 *Mass Spectrometry Reviews*, 26, 185-222, 10.1002/mas.20115, 2007.

678 Charlson, R. J., Langner, J., Rodhe, H., Leovy, C. B., and Warren, S. G.: Perturbation of the northern
679 hemisphere radiative balance by backscattering from anthropogenic sulfate aerosols*, *Tellus B*,
680 43, 152-163, 10.1034/j.1600-0889.1991.t01-1-00013.x, 1991.

681 Cheung, K., Ling, Z. H., Wang, D. W., Wang, Y., Guo, H., Lee, B., Li, Y. J., and Chan, C. K.:
682 Characterization and source identification of sub-micron particles at the HKUST Supersite in
683 Hong Kong, *Science of The Total Environment*, 527–528, 287-296,
684 <http://dx.doi.org/10.1016/j.scitotenv.2015.04.087>, 2015.

685 Crippa, M., DeCarlo, P. F., Slowik, J. G., Mohr, C., Heringa, M. F., Chirico, R., Poulain, L., Freutel, F.,
686 Sciare, J., Cozic, J., Di Marco, C. F., Elsasser, M., Nicolas, J. B., Marchand, N., Abidi, E.,
687 Wiedensohler, A., Drewnick, F., Schneider, J., Borrmann, S., Nemitz, E., Zimmermann, R.,
688 Jaffrezo, J. L., Prévôt, A. S. H., and Baltensperger, U.: Wintertime aerosol chemical composition
689 and source apportionment of the organic fraction in the metropolitan area of Paris, *Atmos. Chem.*
690 *Phys.*, 13, 961-981, 10.5194/acp-13-961-2013, 2013.

691 Davidson, C. I., Phalen, R. F., and Solomon, P. A.: Airborne Particulate Matter and Human Health: A
692 Review, *Aerosol Science and Technology*, 39, 737-749, 10.1080/02786820500191348, 2005.

693 DeCarlo, P. F., Slowik, J. G., Worsnop, D. R., Davidovits, P., and Jimenez, J. L.: Particle morphology
694 and density characterization by combined mobility and aerodynamic diameter measurements. Part
695 1: Theory, *Aerosol Science and Technology*, 38, 1185-1205, 10.1080/027868290903907, 2004.

696 Docherty, K. S., Aiken, A. C., Huffman, J. A., Ulbrich, I. M., DeCarlo, P. F., Sueper, D., Worsnop, D. R.,
697 Snyder, D. C., Peltier, R. E., Weber, R. J., Grover, B. D., Eatough, D. J., Williams, B. J.,
698 Goldstein, A. H., Ziemann, P. J., and Jimenez, J. L.: The 2005 Study of Organic Aerosols at
699 Riverside (SOAR-1): instrumental intercomparisons and fine particle composition, *Atmospheric
700 Chemistry and Physics*, 11, 12387-12420, 10.5194/acp-11-12387-2011, 2011.

701 Drewnick, F., Hings, S. S., DeCarlo, P., Jayne, J. T., Gonin, M., Fuhrer, K., Weimer, S., Jimenez, J. L.,
702 Demerjian, K. L., Borrmann, S., and Worsnop, D. R.: A new time-of-flight aerosol mass
703 spectrometer (TOF-AMS) - Instrument description and first field deployment, *Aerosol Science
704 and Technology*, 39, 637-658, 10.1080/02786820500182040, 2005.

705 Elser, M., Huang, R. J., Wolf, R., Slowik, J. G., Wang, Q., Canonaco, F., Li, G., Bozzetti, C.,
706 Daellenbach, K. R., Huang, Y., Zhang, R., Li, Z., Cao, J., Baltensperger, U., El-Haddad, I., and
707 Prévôt, A. S. H.: New insights into PM_{2.5} chemical composition and sources in two major cities
708 in China during extreme haze events using aerosol mass spectrometry, *Atmos. Chem. Phys.*, 16,
709 3207-3225, 10.5194/acp-16-3207-2016, 2016.

710 Farmer, D. K., Matsunaga, A., Docherty, K. S., Surratt, J. D., Seinfeld, J. H., Ziemann, P. J., and Jimenez,
711 J. L.: Response of an aerosol mass spectrometer to organonitrates and organosulfates and
712 implications for atmospheric chemistry, *Proceedings of the National Academy of Sciences of the
713 United States of America*, 107, 6670-6675, 10.1073/pnas.0912340107, 2010.

714 Gill, P. E., Murray, W., and Wright, M. H.: The Levenberg-Marquardt method, in: *Practical optimization*,
715 Academic Press, London, 1981.

716 Griffith, S. M., Huang, X. H. H., Louie, P. K. K., and Yu, J. Z.: Characterizing the thermodynamic and
717 chemical composition factors controlling PM_{2.5} nitrate: Insights gained from two years of online
718 measurements in Hong Kong, *Atmospheric Environment*, 122, 864-875,
719 <http://dx.doi.org/10.1016/j.atmosenv.2015.02.009>, 2015.

720 Guo, H., Wang, D. W., Cheung, K., Ling, Z. H., Chan, C. K., and Yao, X. H.: Observation of aerosol size
721 distribution and new particle formation at a mountain site in subtropical Hong Kong, *Atmos.
722 Chem. Phys.*, 12, 9923-9939, 10.5194/acp-12-9923-2012, 2012.

723 Huang, X. F., He, L. Y., Hu, M., Canagaratna, M. R., Sun, Y., Zhang, Q., Zhu, T., Xue, L., Zeng, L. W.,
724 Liu, X. G., Zhang, Y. H., Jayne, J. T., Ng, N. L., and Worsnop, D. R.: Highly time-resolved
725 chemical characterization of atmospheric submicron particles during 2008 Beijing Olympic

726 Games using an Aerodyne High-Resolution Aerosol Mass Spectrometer, *Atmospheric Chemistry*
727 *and Physics*, 10, 8933-8945, 10.5194/acp-10-8933-2010, 2010.

728 Huang, X. F., He, L. Y., Hu, M., Canagaratna, M. R., Kroll, J. H., Ng, N. L., Zhang, Y. H., Lin, Y., Xue,
729 L., Sun, T. L., Liu, X. G., Shao, M., Jayne, J. T., and Worsnop, D. R.: Characterization of
730 submicron aerosols at a rural site in Pearl River Delta of China using an Aerodyne High-
731 Resolution Aerosol Mass Spectrometer, *Atmospheric Chemistry and Physics*, 11, 1865-1877,
732 10.5194/acp-11-1865-2011, 2011.

733 Huang, X. H. H., Bian., Q. J., Ng, W. M., Louie, P. K. K., and Yu, J. Z.: Characterization of PM2.5 Major
734 Components and Source Investigation in Suburban Hong Kong: A One Year Monitoring Study,
735 *Aerosol and Air Quality Research* 14, 237-250, 2014.

736 Jayne, J. T., Leard, D. C., Zhang, X. F., Davidovits, P., Smith, K. A., Kolb, C. E., and Worsnop, D. R.:
737 Development of an aerosol mass spectrometer for size and composition analysis of submicron
738 particles, *Aerosol Science and Technology*, 33, 49-70, 2000.

739 Jimenez, J. L., Jayne, J. T., Shi, Q., Kolb, C. E., Worsnop, D. R., Yourshaw, I., Seinfeld, J. H., Flagan, R.
740 C., Zhang, X., Smith, K. A., Morris, J. W., and Davidovits, P.: Ambient aerosol sampling using
741 the Aerodyne Aerosol Mass Spectrometer, *J. Geophys. Res.*, 108, 8425, 10.1029/2001jd001213,
742 2003.

743 John, W.: Size Distribution Characteristics of Aerosols, in: *Aerosol Measurement*, John Wiley & Sons,
744 Inc., 41-54, 2011.

745 Kerminen, V. M., Paramonov, M., Anttila, T., Riipinen, I., Fountoukis, C., Korhonen, H., Asmi, E.,
746 Laakso, L., Lihavainen, H., Swietlicki, E., Svenningsson, B., Asmi, A., Pandis, S. N., Kulmala,
747 M., and Petäjä, T.: Cloud condensation nuclei production associated with atmospheric nucleation:
748 a synthesis based on existing literature and new results, *Atmos. Chem. Phys.*, 12, 12037-12059,
749 10.5194/acp-12-12037-2012, 2012.

750 Köhler, H.: The nucleus in and the growth of hygroscopic droplets, *Transactions of the Faraday Society*,
751 32, 1152-1161, 10.1039/tf9363201152, 1936.

752 Lee, B. P., Li, Y. J., Yu, J. Z., Louie, P. K. K., and Chan, C. K.: Physical and chemical characterization of
753 ambient aerosol by HR-ToF-AMS at a suburban site in Hong Kong during springtime 2011,
754 *Journal of Geophysical Research: Atmospheres*, 118, 8625-8639, 10.1002/jgrd.50658, 2013.

755 Lee, B. P., Li, Y. J., Yu, J. Z., Louie, P. K. K., and Chan, C. K.: Characteristics of submicron particulate
756 matter at the urban roadside in downtown Hong Kong—Overview of 4 months of continuous
757 high-resolution aerosol mass spectrometer measurements, *Journal of Geophysical Research:*
758 *Atmospheres*, 120, 7040-7058, 10.1002/2015JD023311, 2015.

759 Li, Y. J., Lee, B. Y. L., Yu, J. Z., Ng, N. L., and Chan, C. K.: Evaluating the degree of oxygenation of
760 organic aerosol during foggy and hazy days in Hong Kong using high-resolution time-of-flight
761 aerosol mass spectrometry (HR-ToF-AMS), *Atmos. Chem. Phys.*, 13, 8739-8753, 10.5194/acp-
762 13-8739-2013, 2013.

763 Li, Y. J., Lee, B. P., Su, L., Fung, J. C. H., and Chan, C. K.: Seasonal characteristics of fine particulate
764 matter (PM) based on high resolution time-of-flight aerosol mass spectrometric (HR-ToF-AMS)
765 measurements at the HKUST Supersite in Hong Kong, *Atmos. Chem. Phys.*, 15, 37-53,
766 doi:10.5194/acp-15-37-2015, 2015.

767 Liu, P. S. K., Deng, R., Smith, K. A., Williams, L. R., Jayne, J. T., Canagaratna, M. R., Moore, K.,
768 Onasch, T. B., Worsnop, D. R., and Deshler, T.: Transmission efficiency of an aerodynamic
769 focusing lens system: Comparison of model calculations and laboratory measurements for the
770 Aerodyne Aerosol Mass Spectrometer, *Aerosol Science and Technology*, 41, 721-733,
771 10.1080/02786820701422278, 2007.

772 Man, H., Zhu, Y., Ji, F., Yao, X., Lau, N. T., Li, Y., Lee, B. P., and Chan, C. K.: Comparison of Daytime
773 and Nighttime New Particle Growth at the HKUST Supersite in Hong Kong, *Environmental
774 Science & Technology*, 49, 7170-7178, 10.1021/acs.est.5b02143, 2015.

775 Meng, J. W., Yeung, M. C., Li, Y. J., Lee, B. Y. L., and Chan, C. K.: Size-resolved cloud condensation
776 nuclei (CCN) activity and closure analysis at the HKUST Supersite in Hong Kong, *Atmos. Chem.
777 Phys.*, 14, 10267-10282, 10.5194/acp-14-10267-2014, 2014.

778 Mohr, C., DeCarlo, P. F., Heringa, M. F., Chirico, R., Slowik, J. G., Richter, R., Reche, C., Alastuey, A.,
779 Querol, X., Seco, R., Peñuelas, J., Jiménez, J. L., Crippa, M., Zimmermann, R., Baltensperger,
780 U., and Prévôt, A. S. H.: Identification and quantification of organic aerosol from cooking and
781 other sources in Barcelona using aerosol mass spectrometer data, *Atmos. Chem. Phys.*, 12, 1649-
782 1665, 10.5194/acp-12-1649-2012, 2012.

783 Rupakheti, M., Leaitch, W. R., Lohmann, U., Hayden, K., Brickell, P., Lu, G., Li, S. M., Toom-Saunty,
784 D., Bottenheim, J. W., Brook, J. R., Vet, R., Jayne, J. T., and Worsnop, D. R.: An intensive study
785 of the size and composition of submicron atmospheric aerosols at a rural site in Ontario, Canada,
786 *Aerosol Science and Technology*, 39, 722-736, 10.1080/02786820500182420, 2005.

787 Saarikoski, S., Carbone, S., Decesari, S., Giulianelli, L., Angelini, F., Canagaratna, M., Ng, N. L.,
788 Trimborn, A., Facchini, M. C., Fuzzi, S., Hillamo, R., and Worsnop, D.: Chemical
789 characterization of springtime submicrometer aerosol in Po Valley, Italy, *Atmos. Chem. Phys.*,
790 12, 8401-8421, 10.5194/acp-12-8401-2012, 2012.

791 Salcedo, D., Onasch, T. B., Dzepina, K., Canagaratna, M. R., Zhang, Q., Huffman, J. A., DeCarlo, P. F.,
792 Jayne, J. T., Mortimer, P., Worsnop, D. R., Kolb, C. E., Johnson, K. S., Zuberi, B., Marr, L. C.,

793 Volkamer, R., Molina, L. T., Molina, M. J., Cardenas, B., Bernabe, R. M., Marquez, C., Gaffney,
794 J. S., Marley, N. A., Laskin, A., Shutthanandan, V., Xie, Y., Brune, W., Leshner, R., Shirley, T.,
795 and Jimenez, J. L.: Characterization of ambient aerosols in Mexico City during the MCMA-2003
796 campaign with Aerosol Mass Spectrometry: results from the CENICA Supersite, *Atmospheric
797 Chemistry and Physics*, 6, 925-946, 2006.

798 Schwartz, S. E.: The whitehouse effect—Shortwave radiative forcing of climate by anthropogenic
799 aerosols: an overview, *Journal of Aerosol Science*, 27, 359-382, [http://dx.doi.org/10.1016-
800 8502\(95\)00533-1](http://dx.doi.org/10.1016/0021-8502(95)00533-1), 1996.

801 Setyan, A., Zhang, Q., Merkel, M., Knighton, W. B., Sun, Y., Song, C., Shilling, J. E., Onasch, T. B.,
802 Herndon, S. C., Worsnop, D. R., Fast, J. D., Zaveri, R. A., Berg, L. K., Wiedensohler, A.,
803 Flowers, B. A., Dubey, M. K., and Subramanian, R.: Characterization of submicron particles
804 influenced by mixed biogenic and anthropogenic emissions using high-resolution aerosol mass
805 spectrometry: results from CARES, *Atmos. Chem. Phys.*, 12, 8131-8156, 10.5194/acp-12-8131-
806 2012, 2012.

807 Slowik, J. G., Stainken, K., Davidovits, P., Williams, L. R., Jayne, J. T., Kolb, C. E., Worsnop, D. R.,
808 Rudich, Y., DeCarlo, P. F., and Jimenez, J. L.: Particle morphology and density characterization
809 by combined mobility and aerodynamic diameter measurements. Part 2: Application to
810 combustion-generated soot aerosols as a function of fuel equivalence ratio, *Aerosol Science and
811 Technology*, 38, 1206-1222, 10.1080/027868290903916, 2004.

812 Sun, C., Lee, B. P., Huang, D., Jie Li, Y., Schurman, M. I., Louie, P. K. K., Luk, C., and Chan, C. K.:
813 Continuous measurements at the urban roadside in an Asian megacity by Aerosol Chemical
814 Speciation Monitor (ACSM): particulate matter characteristics during fall and winter seasons in
815 Hong Kong, *Atmos. Chem. Phys.*, 16, 1713-1728, 10.5194/acp-16-1713-2016, 2016.

816 Sun, Y., Zhang, Q., Macdonald, A. M., Hayden, K., Li, S. M., Liggio, J., Liu, P. S. K., Anlauf, K. G.,
817 Leaitch, W. R., Steffen, A., Cubison, M., Worsnop, D. R., van Donkelaar, A., and Martin, R. V.:
818 Size-resolved aerosol chemistry on Whistler Mountain, Canada with a high-resolution aerosol
819 mass spectrometer during INTEX-B, *Atmos. Chem. Phys.*, 9, 3095-3111, 10.5194/acp-9-3095-
820 2009, 2009.

821 Sun, Y. L., Zhang, Q., Schwab, J. J., Demerjian, K. L., Chen, W. N., Bae, M. S., Hung, H. M., Hogrefe,
822 O., Frank, B., Rattigan, O. V., and Lin, Y. C.: Characterization of the sources and processes of
823 organic and inorganic aerosols in New York city with a high-resolution time-of-flight aerosol
824 mass spectrometer, *Atmospheric Chemistry and Physics*, 11, 1581-1602, 10.5194/acp-11-1581-
825 2011, 2011.

826 Takegawa, N., Miyakawa, T., Watanabe, M., Kondo, Y., Miyazaki, Y., Han, S., Zhao, Y., van Pinxteren,
827 D., Brüggemann, E., Gnauk, T., Herrmann, H., Xiao, R., Deng, Z., Hu, M., Zhu, T., and Zhang,
828 Y.: Performance of an Aerodyne Aerosol Mass Spectrometer (AMS) during Intensive Campaigns
829 in China in the Summer of 2006, *Aerosol Science and Technology*, 43, 189-204,
830 10.1080/02786820802582251, 2009.

831 Ulbrich, I. M., Canagaratna, M. R., Cubison, M. J., Zhang, Q., Ng, N. L., Aiken, A. C., and Jimenez, J.
832 L.: Three-dimensional factorization of size-resolved organic aerosol mass spectra from Mexico
833 City, *Atmos. Meas. Tech.*, 5, 195-224, 10.5194/amt-5-195-2012, 2012.

834 Westervelt, D. M., Pierce, J. R., Riipinen, I., Trivittayanurak, W., Hamed, A., Kulmala, M., Laaksonen,
835 A., Decesari, S., and Adams, P. J.: Formation and growth of nucleated particles into cloud
836 condensation nuclei: model–measurement comparison, *Atmos. Chem. Phys.*, 13, 7645-7663,
837 10.5194/acp-13-7645-2013, 2013.

838 Williams, L. R., Gonzalez, L. A., Peck, J., Trimborn, D., McInnis, J., Farrar, M. R., Moore, K. D., Jayne,
839 J. T., Robinson, W. A., Lewis, D. K., Onasch, T. B., Canagaratna, M. R., Trimborn, A., Timko,
840 M. T., Magoon, G., Deng, R., Tang, D., de la Rosa Blanco, E., Prévôt, A. S. H., Smith, K. A., and
841 Worsnop, D. R.: Characterization of an aerodynamic lens for transmitting particles greater than 1
842 micrometer in diameter into the Aerodyne aerosol mass spectrometer, *Atmos. Meas. Tech.*, 6,
843 3271-3280, 10.5194/amt-6-3271-2013, 2013.

844 Yao, X., Lau, N. T., Chan, C. K., and Fang, M.: Size distributions and condensation growth of submicron
845 particles in on-road vehicle plumes in Hong Kong, *Atmospheric Environment*, 41, 3328-3338,
846 10.1016/j.atmosenv.2006.12.044, 2007a.

847 Yao, X., Ling, T. Y., Fang, M., and Chan, C. K.: Size dependence of in situ pH in submicron atmospheric
848 particles in Hong Kong, *Atmospheric Environment*, 41, 382-393,
849 10.1016/j.atmosenv.2006.07.037, 2007b.

850 Yuan, Z., Yadav, V., Turner, J. R., Louie, P. K. K., and Lau, A. K. H.: Long-term trends of ambient
851 particulate matter emission source contributions and the accountability of control strategies in
852 Hong Kong over 1998–2008, *Atmospheric Environment*, 76, 21-31,
853 <http://dx.doi.org/10.1016/j.atmosenv.2012.09.026>, 2013.

854 Zhang, J. K., Sun, Y., Liu, Z. R., Ji, D. S., Hu, B., Liu, Q., and Wang, Y. S.: Characterization of
855 submicron aerosols during a month of serious pollution in Beijing, 2013, *Atmos. Chem. Phys.*,
856 14, 2887-2903, 10.5194/acp-14-2887-2014, 2014.

857 Zhang, Q., Stanier, C. O., Canagaratna, M. R., Jayne, J. T., Worsnop, D. R., Pandis, S. N., and Jimenez, J.
858 L.: Insights into the chemistry of new particle formation and growth events in Pittsburgh based on

859 aerosol mass spectrometry, *Environmental Science & Technology*, 38, 4797-4809,
860 10.1021/es035417u, 2004.

861 Zhang, Q., Canagaratna, M. R., Jayne, J. T., Worsnop, D. R., and Jimenez, J. L.: Time- and size-resolved
862 chemical composition of submicron particles in Pittsburgh: Implications for aerosol sources and
863 processes, *Journal of Geophysical Research-Atmospheres*, 110, D07s09 Artn d07s09, 2005.

864 Zheng, M., Kester, D. R., Wang, F., Shi, X., and Guo, Z.: Size distribution of organic and inorganic
865 species in Hong Kong aerosols during the wet and dry seasons, *J. Geophys. Res.*, 113, D16303,
866 10.1029/2007jd009494, 2008.

867 Zhuang, H., Chan, C. K., Fang, M., and Wexler, A. S.: Size distributions of particulate sulfate, nitrate,
868 and ammonium at a coastal site in Hong Kong, *Atmospheric Environment*, 33, 843-853,
869 10.1016/s1352-2310(98)00305-7, 1999.

870